www.nature.com/cdd

CDDpress

ARTICLE

IKBKE phosphorylates and stabilizes Snail to promote breast cancer invasion and metastasis

Wei Xie[1,2,4], Qiwei Jiang[2,4], Xueji Wu[2,4], Lei Wang[2,4], Bing Gao[2], Zicheng Sun[1], Xiaomei Zhang[2], Lang Bu[2], Ying Lin[1], Qiang Huang[3✉], Jie Li[1✉] and Jianping Guo[2✉]

IKBKE, a non-canonical inflammatory kinase, is frequently amplified or activated, and plays predominantly oncogenic roles in human cancers, especially in breast cancer. However, the potential function and underlying mechanism of IKBKE contributing to breast cancer metastasis remain largely elusive. Here, we report that depletion of *Ikbke* markedly decreases polyoma virus middle T antigen (PyVMT)-induced mouse mammary tumorigenesis and subsequent lung metastasis. Biologically, ectopic expression of IKBKE accelerates, whereas depletion of *IKBKE* attenuates breast cancer invasiveness and migration in vitro and tumor metastasis in vivo. Mechanistically, IKBKE tightly controls the stability of transcriptional factor Snail in different layers, in particular by directly phosphorylating Snail, which markedly blocks the E3 ligase β-TRCP1-mediated Snail degradation, resulting in breast cancer epithelial-mesenchymal transition (EMT) and metastasis. These findings together reveal a novel oncogenic function of IKBKE in promoting breast cancer metastasis by governing Snail abundance, and highlight the potential of targeting IKBKE for metastatic breast cancer therapies.

Cell Death & Differentiation (2022) 29:1528–1540; https://doi.org/10.1038/s41418-022-00940-1

INTRODUCTION

Update to 2020, breast cancer remains the first occurrence of estimated new cancer cases (30% of total cancers) and second cause of cancer mortality (15% of total cancer death) among women in the United States [1]. The determinant of mortality in breast cancer patients is mainly due to the tumor metastasis, including but not limited to the region of lymph nodes, lungs, bone and brain [2, 3]. Among breast cancers, triple negative breast cancer (TNBC), commonly occurs among young ages and spreads in the early stage, leading to inefficient therapies, especially for targeted therapies [4]. As such, much effort has been devoted to discover how metastasis develops in breast cancers, including identification of genetic alterations or dysregulated signaling pathways that determine metastatic potency raised from non-dominant cells within primary tumors [5, 6]. These findings will provide potent strategies for the diagnosis, prognosis and target therapies of metastatic breast cancer.

Being considered as an important cause of cancer, chronic inflammation occurs in several malignancies, especially in cervical, gastric cancer and hepatocarcinoma [7–9]. Specifically, the classical inflammatory kinases, including IKKα and IKKβ, and their downstream NF-κB signal, are naturally highly associated with tumorigenesis [10]. Recently, via high through-put screening approaches, two non-canonical inflammatory kinases, IKBKE and TBK1 have been identified to play pivotal oncogenic roles in breast and lung tumorigenesis, respectively [11, 12]. More importantly, the oncogenic roles of IKBKE and TBK1 are not only limited to the activation of inflammation and innate immune response by activating NF-κB and IRF3/7 pathways, but also directly enabling other oncogenic hubs such as the AKT kinase and the YAP transcriptional factor in a phosphorylation-dependent manner, contributing to tumorigenesis [13–15]. Structurally, IKBKE exhibits more sequence homology with TBK1 than IKKα and IKKβ [11], in addition, IKBKE displayed similar but not identical with TBK1 by phosphorylating various overlapped and distinct substrates [16]. Meanwhile, considered as an inducible kinase, IKBKE could be transcriptionally induced by various inflammatory factors, such as PMA and LPS [17, 18], and transduces immune response by activating STAT1 or IRF3/7 pathway [19, 20]. Recently, IKBKE has also been identified as a potential prognosis biomarker for the diagnosis of ovarian and lung cancer patients [21, 22]. Interestingly, the novel roles of IKBKE in TNBC have also been evaluated by activating STAT3-mediated cytokine networks or manipulating TRAF2 activity [23, 24]. Although IKBKE has been considered for regulating breast cancer migration [25], how IKBKE contributes to breast cancer metastasis, especially in mouse models is not defined yet.

Epithelial-mesenchymal transition (EMT), a progress that epithelial cells acquire fibroblast-like properties by reducing intercellular adhesion and increasing motility, has been considered as a hallmark of motility and invasiveness of tumor cells [26, 27]. More importantly, it's believed that EMT also contributes to cancer chemoresistance and cancer stem cells (CSCs) sustention, and plays important roles in tumor recurrence and metastasis

[1]Department of Breast and Thyroid Surgery, the First Affiliated Hospital, Sun Yat-sen University, Guangzhou, Guangdong 510275, China. [2]Institute of Precision Medicine, the First Affiliated Hospital, Sun Yat-sen University, Guangzhou, Guangdong 510275, China. [3]Department of Neurosurgery, Tianjin Medical University General Hospital, Tianjin 300052, China. [5]These authors contributed equally: Wei Xie, Qiwei Jiang, Xueji Wu, Lei Wang. ✉email: huangqiang209@163.com; Lijie78@mail.sysu.edu.cn; guojp6@mail.sysu.edu.cn

Edited by K Newton

Received: 30 June 2021 Revised: 10 January 2022 Accepted: 12 January 2022
Published online: 22 January 2022

[28, 29]. Accumulating evidence indicates that several transcription factors, such as Snail/Slug, Twist and dEF1/ZEB1 are predominantly implicated in the control of EMT [26, 27], among which Snail has been demonstrated as one of the most important central regulators of epithelial cell adhesion during embryo development [30]. Due to its central roles in governing EMT, Snail undergoes a tightly governing manner, such as in the levels of miRNAs-mediated post-transcriptional control [31, 32] or kinases (such as GSK-3β, PAK1 and PKD1)-mediated post-translational modifications [33–35].

In this study, we reveal the dominant roles of IKBKE in breast cancer metastasis, and demonstrate that *Ikbke* depletion prevents *MMTV-PyVMT* mouse mammary epithelial hyperplasia and tumor formation, as well as remarkably decreases or delays mammary tumor lung metastasis. Biologically, IKBKE could promote breast cancer cell EMT and metastasis by stabilizing Snail, largely in a phosphorylation dependent manner, which proposes a potential strategy to combat breast cancer invasion and metastasis by targeting IKBKE.

MATERIALS AND METHODS

Cell culture and transfection

HEK293, HEK293T cells and mouse mammary immortalized cell NmuMG were cultured in DMEM medium supplemented with 10% FBS. Breast cancer cell lines including MCF7 and MDA-MB231 were culture in MEM medium or L15 medium supplemented with 10% FBS. Human breast MDA-MB-231 cells with lung metastatic potential and luciferase (MDA-MB231-Luc-D3H2LN) were cultured in DMEM medium (as a gift from Dr. Junchao Cai, Sun Yat-sen University). HEK293-sgAKT1 cell line were generated via a CRISPR/CAS9 method as described before [36].

Cell transfection was performed as described previously [36]. Lentiviral encoding or shRNA virus packaging and subsequent infection were performed according to the protocols described previously [36]. Following viral infection, cells were maintained in the presence of hygromycin (200 μg/ml) or puromycin (1 μg/ml), depending on the viral vectors used to infect cells.

Insulin (Invitrogen 41400-045), Mk2206 (Selleck, S1078), NF-κB inhibitor QNZ (Selleck, S4902), TNFα (R&D, 210-TA-005), MG132 (Selleck, S2619), Cycloheximide (CHX) (MCE, HY-12320), Compound 1 (COMP1) (Selleck, S8922) were used at the indicated doses.

Plasmid construction

The pCMV-Myc tagged IKBKE, Myc-myr-IKBKE and Myc-DN-IKBKE-K38A were described previously [11]. β-TRCP1 construct was obtained from Dr. Wei lab at BIDMC, Harvard Medical School. Flag-Snail, CMV-GST-Snail, pGEX-4T1-Snail were constructed by sub-cloning the Snail cDNA into pCDNA3-Flag, pCMV-GST and pGEX-4T-1, respectively. Snail-S165A and -S165D mutants were obtained via Q5 Site-Directed Mutagenesis Kit (New England Biolabs) according to the manufacturer's instructions.

Antibodies

Anti-Ki67 (ab16667) and anti-thiophosphate ester (ab92570) antibodies were purchased from Abcam. Anti-Cleaved Caspase3 (#9579), anti-IKBKE (#3416), anti-E-Cadherin (#14472), anti-Myc-tag (#2276), anti-Snail (#3879), anti-N-Cadherin (#13116), anti-Vimentin (#5741), anti-AKT1 (#75692), anti-GSK-3β (#12456), anti-ZO-1 (#13663) and anti-GST (#2625) antibodies were purchased from Cell Signaling. Anti-Actin antibody (sc-69879) was purchased from Santa Cruz. Anti-GAPDH antibody (60004-1-Ig) was purchased from Proteintech. Anti-Flag (F1804, clone M2) and anti-Vinculin (V4505) antibodies were purchased from Sigma. Peroxidase-conjugated anti-mouse secondary antibody (115-035-003) and anti-rabbit secondary antibody (111-035-003) were purchased from Jackson. Anti-pS165-Snail poly-antibodies were generated by ABclonal with the peptide NKEYL(pS)LGALK as antigen.

Immunoprecipitation, GST pull-down assays and western blot

Cells were lysed in EBC buffer (50 mM Tris pH 7.5, 120 mM NaCl, 0.5% NP-40) supplemented with protease inhibitors (cOmplete™ Protease Inhibitor Cocktail, Roche) and phosphatase inhibitors (PhosSTOP, Roche). The protein concentrations of whole cell lysates were measured by Pierce™ BCA Protein Assay Kit (23225). Equal amounts of whole cell lysates were resolved by SDS-PAGE and immunoblotted with indicated antibodies. For immunoprecipitation, 1000 μg lysates were incubated with the indicated antibody (1–2 μg) for 3–4 h at 4 °C followed by 1 h incubation with Protein A/G sepharose beads (GE Healthcare). For GST pull-down assays, 1000 μg lysates were incubated with glutathione sepharose 4B (GE Healthcare) for 2 h at 4 °C. The immunoprecipitants were washed five times with NETN buffer (20 mM Tris, pH 8.0, 150 mM NaCl, 1 mM EDTA and 0.5% NP-40) before being resolved by SDS-PAGE and immunoblotted with indicated antibodies. All antibodies were used at a 1:1000 dilution in TBST buffer with 5% BSA for western blot. Quantification of the immunoblot band intensity was performed with Image J software.

In vivo ubiquitination assay

HEK293T cells were transfected with His-Ub and the indicated constructs. Thirty-six hours after transfection, cells were treated with 10μM MG132 for 12 h and washed with PBS twice, and then were lysed in buffer A (6 M guanidine-HCl, 0.1 M Na_2HPO_4/NaH_2PO_4, and 10 mM imidazole [pH 8.0]) and subjected to sonicate. After high-speed centrifuged, the supernatants were incubated with nickel-beads (Ni-NTA) (QIAGEN) for 3 h at room temperature. The products were washed twice with buffer A, twice with buffer A/TI (1 volume buffer A and 3 volumes buffer TI), and one time with buffer TI (25 mM Tris-HCl and 20 mM imidazole [pH 6.8]). The pull-down proteins were resolved in 10% SDS-PAGE for immunoblot analysis.

Immunofluorescence staining

Briefly, cells grown on glass coverslips were fixed in methanol at −20 °C for 20 m, blocked with 10% goat serum, and then incubated with primary antibodies (1:200) targeting Snail, E-cadherin, Vimentin and ZO-1 overnight at 4°C, washed thrice with PBS, and then incubated with 546 Alexa (red)-labeled secondary antibodies (Molecular Probes, Orlando, FL). The DNA dye DAPI was used to counterstain the nuclear DNA.

In vitro kinase assays

IKBKE in vitro kinase assay was performed as previously described [37, 38]. Briefly, the reaction was carried out in the presence of 100 ng ATP-γ-S (ab138911) and 200 μM cold ATP in 30 μl kinase buffer containing 50 mM Tris (pH 7.5), 10 mM $MgCl_2$ and 2 mM DTT. After incubation at 30 °C for 30 min, the reaction was stopped by adding in final concentration of 0.1 mM EDTA, and then p-Nitrobenzyl mesylate (ab138910) was used to alkylate the thiophospholyation site on the substrates. The reaction was stopped by adding SDS loading buffer and then subjected to western blot assay. Anti-Thiophosphate ester antibody (ab92570) was used to identify the tagged substrates.

Breast cancer tissues, TMA and IHC staining

Breast cancer tissues were obtained from Department of Breast and Thyroid Surgery at the First Affiliated Hospital, Sun Yat-sen University. Tissue array (BC081120d) containing 10 cases of adjacent normal breast tissues, 100 cases of ductal carcinoma were obtained from Biomax. The mammary and lung tissue samples from mice were fixed in 10% neutral buffered formalin, embedded in paraffin, and cut into 4 μm sections. These samples were deparaffinized, rehydrated, and subjected to heat-mediated antigen retrieval. The tissue sections were stained with hematoxylin-eosin (H&E). For IHC staining, the sections were incubated with 3% H_2O_2 for 15 min and protein blocking reagents (Dako #X0909) for 5 m. Sections were then incubated with indicated antibodies diluted in Dako diluent with background reducing components (Dako#S3022) for 1 h at room temperature. Following primary antibody incubation for IKBKE (Sigma, 1:200), pS165-Snail (ABclonal, 1:100), sections were incubated with monoclonal mouse anti-rabbit immunoglobulins (Dako#M0737) for 30 min at room temperature. Afterwards, sections were incubated with Envision+ System-HRP Labeled Polymer Anti-Rabbit (Dako #K4003) for 30 min. All sections were developed using the DAB chromogen kit (Dako#K3468) and lightly counterstained with hematoxylin.

Purification of GST-tagged proteins from bacteria

Recombinant GST-conjugated Snail was generated by transforming the BL21 (DE3) *E. coli* strain. Starter cultures (5 ml) grown overnight at 37 °C were inoculated (1%) into larger volumes (500 ml). Cultures were grown at 37 °C until an O.D. of 0.8, following which protein expression was induced for 12–16 h using 0.1 mM IPTG at 16 °C with vigorous shaking. Recombinant proteins were purified from harvested pellets. Pellets were re-suspended in 5 ml EBC buffer and sonicated. Insoluble proteins and cell

debris were discarded following centrifugation in a table-top centrifuge (13000 rpm/4 °C/15 min). Each 1 ml supernatant was incubated with 50 µl of 50% Glutathione-sepharose slurry (Pierce) for 3 h at 4 °C. The Glutathione beads were washed 3 times with PBS buffer and eluted by elution buffer. The purified proteins were analyzed by coomassie blue staining and quantified with BSA standards.

Mass spectrometry analyses

Mass spectrometry was used to map the phosphorylation sites of Snail by IKBKE as previously reported [36]. After separation of in vitro IKBKE/Snail kinase reactions in SDS-PAGE, Snail bands were excised and washed. Proteins were reduced with Tris(carboxyethyl) phosphine and alkylated with iodoacetamide. Samples were digested overnight with modified sequencing grade trypsin (Promega, Madison, WI). Peptides were extracted and concentrated under vacuum centrifugation. A nanoflow liquid chromatograph (U3000, LC Packings/Dionex, Sunnyvale, CA) coupled to an electrospray hybrid ion trap mass spectrometer (LTQ Orbitrap, Thermo, San Jose, CA) was used for tandem mass spectrometry peptide sequencing. Sequences were assigned using Mascot data base searches. Phosphorylated serine, threonine, and tyrosine were selected as variable modifications, and as many as 2 missed cleavages were allowed. Assignments were manually verified by inspection of the tandem mass spectra and coalesced into Scaffold.

Quantitative RT-PCR

Total RNA was isolated from the cells using TRIzol Reagent (Invitrogen), and 1 µg of each RNA sample was reverse transcribed to cDNA which was subsequently analyzed by quantitative PCR. All reactions were carried out in triplicate. Relative gene expression was calculated using the $2^{-\Delta\Delta Ct}$ method. Housekeeping gene glyceraldehyde-3-phosphate dehydrogenase (GAPDH) was used as internal controls to normalize target mRNA expression. Primer sequences used were E-cadherin forward (5′-GG CCTGAAGTGACTCGTAACGA-3′) and reverse (5′-GCTCAGACTAGCAGCTTCG GAAC-3′), N-cadherin forward (5′-CCTGCTTATCCTTGTGCTGA-3′) and reverse (5′-CCTGGTCTTCTTCTCCTCCA-3′), Vimentin forward (5′-CAAAGCAG GAGTCCACTGAG-3′) and reverse (5-TAAGGGCATCCACTTCACAG-3′), Snail forward (5′-CACATCCGAGTGGGTTTGG-3′) and reverse (5′-CCACTGCAACC GTGCTTTT-3′), or GAPDH forward (5′-CATGTTCGTCATGGGTGTGAACCA-3′) and reverse (5′-AGTGATGGCATGGACTGTGGTCAT-3′).

Wound healing and trans-well invasion assays

Would healing assays were carried out as previously described [39]. In vitro invasion assays were performed using 6-well, 8 µm pore trans-well inserts (Becton Dickinson). Cells were first resuspended in Matrigel (Becton Dickinson) for invasion assays. We seeded 5×10^4 cells in 200 µl of serum-free growth medium in the upper chamber, and 600 µl of medium with chemo-attractant (10% FBS) was added to the lower chamber. Cells were incubated at 37 °C for 24 h, then fixed in 10% (wt/vol) buffered formalin and stained with 0.05% crystal violet (Sigma). Cells on the upper surface were removed with a cotton swab, and migrated cells on the underside were counted (average of 10 fields/trans-well).

Flow cytometry analysis

For CD44/CD24 flow cytometry analysis, resuspend cells in PBS containing 2% BSA at the density of 1×10^6 incubated with CD44-PE (BD, 1:50 dilution) and CD24-APC (BD, 1:50 dilution) antibody. After washed twice with PBS containing 2% BSA, resuspend cells in 500 ul PBS and subjected for flow cytometry analyses.

Mammosphere formation assays

3000 cells/well were plated into 12-well ultra-low attachment plates (Corning) in serum-free mammary cell growth medium (MammoCult Media, STEMCELL Technologies). Fresh media were changed every 4 days. Floating sphere that grew in 1–2 weeks were counted and taken pictures. Under each condition, experiment was determined in triplicated. Results were representative of three independent experiments.

Mouse assays

FVB/N-Tg(*MMTV-PyVMT*)-transgenic mice and B6.Cg ($Ikbke^{-/-}$)^{tm1Tman} mice were obtained from the Jackson Laboratory. These mice were housed in a specific pathogen-free environment. We took a stepwise strategy to generating female *MMTV-PyVMT/Ikbke*$^{-/-}$ mice and *MMTV-PyMT/Ikbke*$^{+/+}$mice with C57BL/6 background; the offspring were genotyped by PCR of genomic DNA derived from tail clippings. Only virgin female mice were used for experiments, in which 100% of *PyVMT/Ikbke*$^{+/+}$ mice developed mammary carcinomas. For the assessment of multifocal dysplastic lesions, young mice between the ages of 4 and 8 weeks were used. For the evaluation of palpable tumor onset, the mice were monitored twice weekly for mammary tumors by palpating. For histologic analysis, sections of tumors and inflated lungs were fixed in 10% buffered formalin, embedded and stained.

For tail vein injections, 1×10^6 cells were injected, and mice were sacrificed six weeks post-injection. For orthotopic injection, 5×10^6 cells were injected into the left #4 mammary fat pad of anesthetized (isofluorane) nu/nu mice (Sun Yat-sen University). Mice were monitored twice weekly for tumor growth. Animals were killed when tumors reached a mean cross-sectional area of 400 mm^3.The number of lungs with surface metastases were determined, as well as the number of surface metastases per lung by examination under a dissecting microscope, as described elsewhere.

For COMP1 treatment experiments, mice bearing tail-vein injected cells were imaged and separated into two comparable groups (8 mice/group). The lung image was monitored once/three days. The inhibitor COMP1 (15 mg/kg, once/three days, oral) or the vehicle was administrated. 32 days after injection, the mice were sacrificed and subjected for lung tumor staining.

Ethics statement

All experimental procedures were approved by the Institutional Animal Care & Use Committee (IACUC, RN150D) at Sun Yat-sen University with protocol. The research projects that are approved by the IACUC are operated according to the applicable Institutional regulations. The Institute is committed to the highest ethical standards of care for animals used for the purpose of continued progress in the field of human cancer research.

Statistics

Differences between control and testing cells were evaluated by Student's *t* test. For mice tumor formation analysis were carried out by Kaplan-Meier curve (Log-rank test at < 0.05). The correlation of IKBKE expression with L.N. and Snail phosphorylation was analyzed with Chip-square analysis. These analyses were performed using the Prism 7 Software and $p < 0.05$ was considered statistically significant.

RESULTS

Depletion of *Ikbke* attenuates MMTV-PyVMT-induced mouse mammary tumorigenesis and lung metastasis

Although the oncogenic role of IKBKE in promoting breast tumorigenesis has been well established by activating the NF-κB signal [11], whether and how IKBKE modulates breast tumor invasion and metastasis are not well defined. To this end, we initially assessed the physiological functions of *Ikbke* in mouse mammary development by depletion of *Ikbke*, and could not observe detectably impaired mouse mammary gland development. By contrast, depleting *Ikbke* significantly decreased PyVMT-induced mammary tumor genesis and development, indicated by the hyperplastic nodule formation in the mammary glands of mice (Fig. 1A). Interestingly, the mammary ductal cells derived from MMTV-*PyVMT;Ikbke*$^{-/-}$ (termed as *PyVMT;Ikbke*$^{-/-}$) mice displayed proliferative disadvantage indicated by the staining of proliferative marker Ki67, at as early as 4 weeks after birth compared with those derived from *PyVMT;Ikbke*$^{+/+}$ mice (Fig. 1B). In keeping with this notion, *Ikbke* knockout dramatically prolonged the onset time for mammary tumors derived from *PyVMT;Ikbke*$^{-/-}$ mice compared with those from *PyVMT;Ikbke*$^{+/+}$ mice (93 days *versus* 68 days, Fig. 1C), coupled with a markable reduction of tumor numbers (Fig. 1D). In addition, the mammary tumors derived from *PyVMT;Ikbke*$^{-/-}$ mice exhibited a lower proliferation (Ki-67) and higher apoptosis (cleaved Caspase 3) features compared with those derived from *PyVMT;Ikbke*$^{+/+}$ mice (Fig. 1E, F).

To further reveal the malignant functions of IKBKE in vivo, we observed that the lung metastases of mammary tumors were compromised around four times in *PyVMT;Ikbke*$^{-/-}$ mice compared with *PyVMT;Ikbke*$^{+/+}$ mice (Fig. 1G, H). Notably, compared with

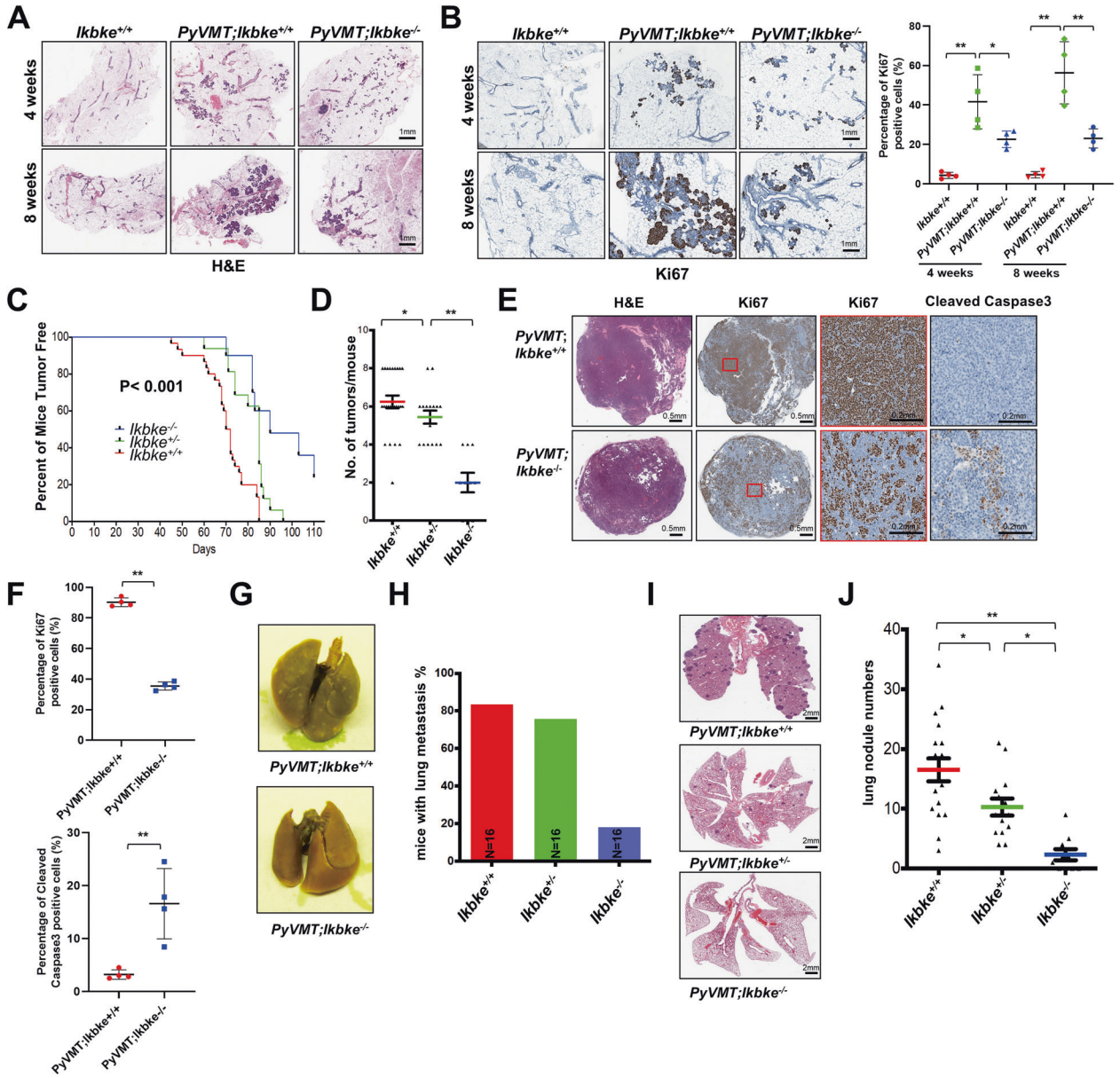

Fig. 1 Depletion of *Ikbke* reduces PyVMT-induced mammary tumorigenesis and lung metastasis. A, **B** Mammary tissues derived from WT or PyVMT transgene mice crossed with or without *Ikbke*$^{-/-}$mice (6 mice/group) were stained with H&E (**A**) or Ki67 (**B**, lef panel). The staining of Ki67 was further quantified (B, right panel). Data are expressed as mean ± SD. *$p < 0.05$, ** $p < 0.01$ (Student *t* test). **C** The percentage of mice with mammary tumors was calculated and illustrated based on the mammary tumor formation among PyVMT transgene mice crossed with or without *Ikbke*$^{-/-}$mice (20 mice/group). **D** The mammary tumor numbers derived from (**C**) were calculated after born 80 days and plotted. Data are expressed as mean ± SD. *$p < 0.05$, ** $p < 0.01$ (Student *t* test). **E**, **F** Mammary tumors derived from PyVMT transgene mice crossed with or without *Ikbke*$^{-/-}$ mice (6 mice/group) were dissected after born 80 days and subjected for staining with indicated antibodies (**E**), which was further quantified (**F**). Data are expressed as mean ± SD. *$p < 0.05$, ** $p < 0.01$ (Student *t* test). **G** Lung tissues were obtained from PyVMT transgene mice crossed with or without *Ikbke*$^{-/-}$ mice after born 90 days (16 mice/group). **H** The lung metastasis of mammary tumor-derived from (**G**) were calculated and presented. **I** Lung tissues derived from (**G**) were dissected and stained with H&E (**I**), and the mammary tumor lung metastasis nodules were calculated and plotted (**J**). Data are expressed as mean ± SD. *$p < 0.05$, **$p < 0.01$ (Student *t* test).

Ikbke-wild type (WT) mice, *Ikbke*- knock-out (KO) mice exhibited a significant decrease in lung nodules formation (Fig. 1I, J). These findings together demonstrate that IKBKE also plays a pivotal role in promoting PyVMT-induced mammary tumor initiation, progression, and lung metastasis.

IKBKE promotes breast cancer cell invasion, migration, and lung metastasis

To further validate the migratory and invasive properties of IKBKE in breast cancer, we knocked down *IKBKE* in breast cancer MDA-MB-231-luc cells, and observed that decrease of *IKBKE* not only repressed cell growth (Figure S1A), but also markedly reduced cell migration and invasion capabilities compared with the counterpart cells (Fig. 2A–C, Figure S1B, C). Consistent with the previous findings that IKBKE serves as an oncoprotein in breast cancer [11], depletion of *IKBKE* reduced the tumor formation in orthotopic mouse models (Fig. 2D, E, Figure S1D). More interestingly, mice bearing *IKBKE*-deficient tumors also exhibited a lesser extent of mammary tumor lung metastasis (Fig. 2F, G, S1E). To further verify the metastatic feature of *IKBKE*-deficient cells, we employed a tail-vein injection mouse model (Fig. 2H), and observed that depleting *IKBKE* alleviated MDA-MB-231 cells lung translocation (Fig. 2I–K).

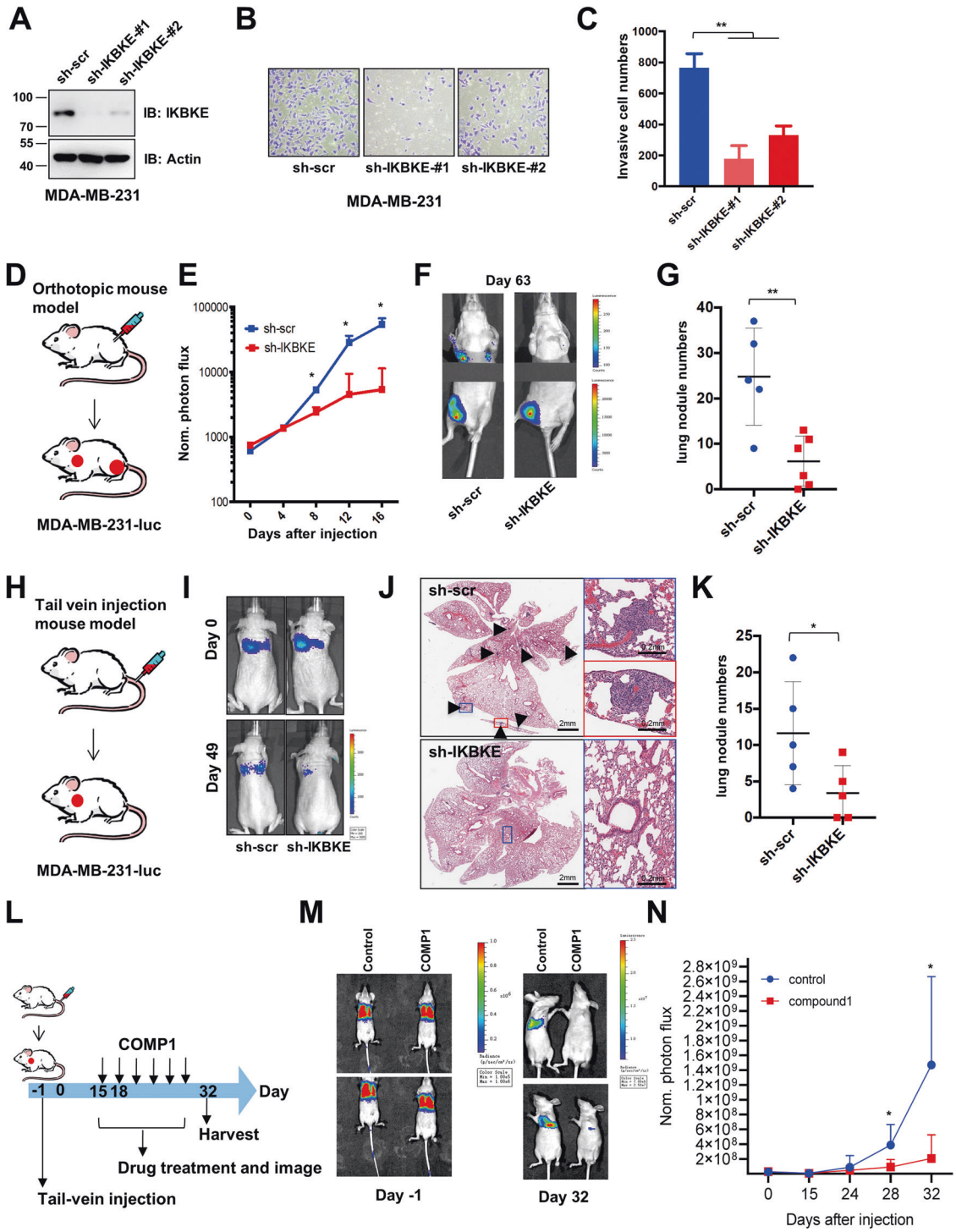

These data together evidence that *IKBKE* depletion not only abrogates breast tumor formation, but also predominantly attenuates breast tumor lung metastasis.

To investigate whether the kinase activity is essential for IKBKE modulating breast cancer cell lung metastasis, IKBKE/TBK1 specific inhibitor Compound 1 (COMP1) was employed [40], which could dramatically decrease breast cancer cell lung metastasis (Fig. 2L–N), coupled with decreased tumor cell proliferation (Fig. S1F, G). Since COMP1 also targets IKBKE cousin protein TBK1 [40], to validate the important roles of IKBKE in mediating breast cancer malignancies, we depleted *IKBKE* in breast cancer cells (Figure S1H), and observed that COMP1 administration could only attenuate intact but not *IKBKE* deficiency-induced cell invasion and migration phenotypes (Figure S1I–L). This finding indicates that COMP1 represses cancer cell malignancies mainly via targeting IKBKE kinase. Next, we ectopically expressed constitutively active IKBKE (Myr-IKBKE) in breast cancer MCF7 cells (Figure S2A). The results showed that ectopic expression of IKBKE could strongly enhance cell invasion and migration assessed with wound healing and trans-well migratory assays (Figure S2B–E), suggesting that high expression of IKBKE could promote breast cancer malignant phenotypes.

Fig. 2 Knockdown of *IKBKE* compromises breast cancer malignant phenotypes. A MDA-MB-231-luc cells were infected with independent shRNAs against *IKBKE*, and selected with puromycin (1 μg/ml) for 72 h, then harvested for Immunoblot (IB) analysis. **B** Resulting cells were subjected to Matrigel-based invasion assays. **C** The invasive cell numbers were calculated and plotted. Experiment was determined in triplicated. Results were representative of three independent experiments. Data are expressed as mean ± SD. $^{**}p < 0.01$ (Student *t* test). **D** Cells generated in (**A**) were subjected to orthotopic assays by injecting cells into the mammary tissues as indicated (6 mice/group). **E** The photon flux of the tumor luciferase was monitored each 4 days. $^{*}p < 0.05$ (Student *t* test). **F** The photon flux of the tumor luciferase derived from mammary or lung were imaged after injecting the cells for 63 days. **G** At that time, the lung tissues were dissected and stained with H&E to measure the mammary tumor lung metastasis by calculating the tumor nodules and plotted. Data are expressed as mean ± SD. $^{**}p < 0.01$ (Student *t* test). **H** Cells generated in (**A**) were subjected to tail-vein injection assays by tail vein injecting the cells into the nude mice as indicated (6 mice/group). **I** The photon flux of the tumor luciferase was monitored in day 0 and 49 after injecting the cells. **J** At that time, the lung tissues were dissected, and H&E staining was performed. **K** Mammary tumor lung metastasis nodules were calculated and plotted. Data are expressed as mean ± SD. $^{*}p < 0.05$ (Student *t* test). **L**–**N** MDA-MB-231-luc cells were used for tail-vein injection assays and then subjected for COMP1 administration assays (**L**). After that, mice bearing tumor cells were divided into two comparable groups dependent on the intension of photon flux after tail-vein injection (day -1) (8 mice/group). After another 15 days, COMP1 (15 mg/kg) and vehicle were orally administrated every 3 days (**L**), the photon flux of the tumor luciferase was monitored in day -1 and 32 after injecting the cells (**M**, **N**). Data are expressed as mean ± SD. $^{*}p < 0.05$ (Student *t* test).

IKBKE promotes EMT process and results in cancer stem cell maintenance

It's well known that epithelial cell transfers to the invasive and migrative phenotype mainly via an epithelial-mesenchymal transition (EMT) process [26]. Thus, we intended to detect whether IKBKE induced breast cancer metastasis was realized by promoting the cellular EMT. To this end, we initially employed a mouse mammary cell line NmuMG, and observed that enforcing expression of IKBKE could strongly decrease the epithelia markers E-cadherin and ZO-1 expression, whereas increase the mesenchymal marker Snail and Vimentin expression (Fig. 3A). Consistent with these findings, ectopically expressing constitutively active, but not kinase dead (DN, K23A) IKBKE decreased E-cadherin expression, coupled with increased N-cadherin, Vimentin and Snail expression (Fig. 3B). To further reveal the potential mechanism of IKBKE in promoting EMT, we detected the mRNA levels of EMT markers and observed that active IKBKE significantly down-regulated *E-cadherin*, while upregulated *N-cadherin* and *Vimentin* expression, but mildly influenced *Snail* expression (Fig. 3C). In keeping with this notion, depletion of *IKBKE* could markedly modulate these EMT markers (Fig. 3D). These observations together illustrate that IKBKE regulates EMT possibly by regulating Snail abundance, leading to Snail-dependent transcriptional control of other EMT markers such as E-cadherin, N-cadherin, and Vimentin [30].

EMT is considered as an important driver event for stem cell initiation and maintenance [29], and the breast cancer stem cell (BCSC) has been reported an close association with cell metastasis and EMT processing [41]. Although the potential role of IKBKE in regulating BCSC has been recently reported [42], here we observed that enforcing expression of active IKBKE enhanced the side population cells of $CD44^{postive}/CD24^{negative}$, specific biomarker of BCSC (Fig. 3E, F) in MCF7 cells [43]. We further hypothesized that IKBKE might control BCSC traits via governing the EMT process. In support of this model, we found that IKBKE dramatically enhanced BCSC traits such as sphere formation (Fig. 3G, H). Consistent with these findings, depletion of *IKBKE* could robustly decrease the side population of $CD44^{postive}/CD24^{negative}$ (Fig. 3I, J) and sphere formation (Fig. 3K, L) in MDA-MB-231 cells. These findings coherently suggest that IKBKE plays an important role in sustaining BCSC characteristics.

IKBKE stabilizes Snail partially by activating AKT/GSK-3β and NF-κB signals

Since IKBKE elevates Snail in protein level, but not mRNA level (Fig. 3B, C), we hypothesized that IKBKE regulated Snail protein at the post-translational level. To test this hypothesis, we detected Snail protein half-life, and observed that the presence of active, but not kinase-dead, IKBKE could dramatically prolong Snail half-life (Fig. S3A, B). Inconsistent with this finding, depletion of IKBKE could markedly repress Snail half-life (Fig. 4A, B). To assess whether IKBKE could regulate Snail ubiquitination, we performed in vivo ubiquitination assays and observed that the active form but not DN form of IKBKE compromised Snail ubiquitination (Fig. 4C). On the other hand, depletion of *IKBKE* resulted in endogenous Snail ubiquitin conjugation (Fig. 4D). To further study the potential function of IKBKE kinase activity, shortened Snail half-life and elevated ubiquitin conjugation were observed upon administration of IKBKE inhibitor COMP1 (Fig. 4E–G, S3C, D). These data together imply that IKBKE promotes Snail stability by decreasing its ubiquitination and degradation.

It is previously reported that two major signaling pathways are defined in governing Snail protein stability. One is GSK-3β-mediated Snail phosphorylation and degradation [33], the other is NF-κB/CSN2 axis-mediated regulation of Snail E3 ligase β-TRCP1 [44]. Since AKT has been validated as a direct substrate of IKBKE [13, 14], and could directly phosphorylate and inhibit GSK3β [45], thus, we first asked whether IKBKE stabilized Snail via manipulating AKT/GSK3β-mediated Snail degradation. To this end, we observed that depletion of *AKT1* only partially decreases IKBKE-induced Snail protein stability (Fig. 4H). Notably, depletion of the *IKBKE*-mediated decrease of Snail could be only mildly rescued by activating AKT via insulin stimulation (Fig. 4I). Moreover, GSK3β, a major target of AKT in regulating Snail, and its active form GSK-3β-S9A only mildly decreased IKBKE-induced Snail stabilization (Fig. S3E). Collectively, our observations indicate that IKBKE stabilizes Snail only partially depending on its modulation of AKT/GSK-3β signaling.

In addition, NF-κB pathway was also reported to play an important role in stabilizing Snail toward inflammatory stimuli [44]. As a member of IκB kinase, IKBKE was clearly demonstrated to activate NF-κB pathway in various ways [37, 46], so we sought to detect whether IKBKE induced Snail stabilization was mediated by the NF-κB/CSN2 pathway. To this end, we found that TNFα, but not IKBKE, increased Snail abundance had been abrogated by blocking the NF-κB pathway via transfected the supper-inhibitor IκBα-DN (Fig. 4J) [47]. More importantly, repressing both AKT and NF-κB pathways by knocking out *AKT1* and treating with NF-κB inhibitor QNZ, only partially decreased IKBKE-induced Snail abundance (Fig. 4K), indicating that except AKT/GSK3 and NF-κB pathways, other ways are involved in IKBKE regulating Snail stability (Fig. 4L).

IKBKE directly phosphorylates and stabilizes Snail

To investigate the connection of IKBKE with Snail, we observed that IKBKE interacted with Snail both in cells (Fig. 5A, S4A, B) and in vitro (Fig. 5B). As a serine/threonine kinase, IKBKE has been reported to phosphorylate many downstream substrates [16], so we tended to confirm whether IKBKE could directly phosphorylate Snail. To this end, we performed in vitro kinase assays and found that IKBKE could

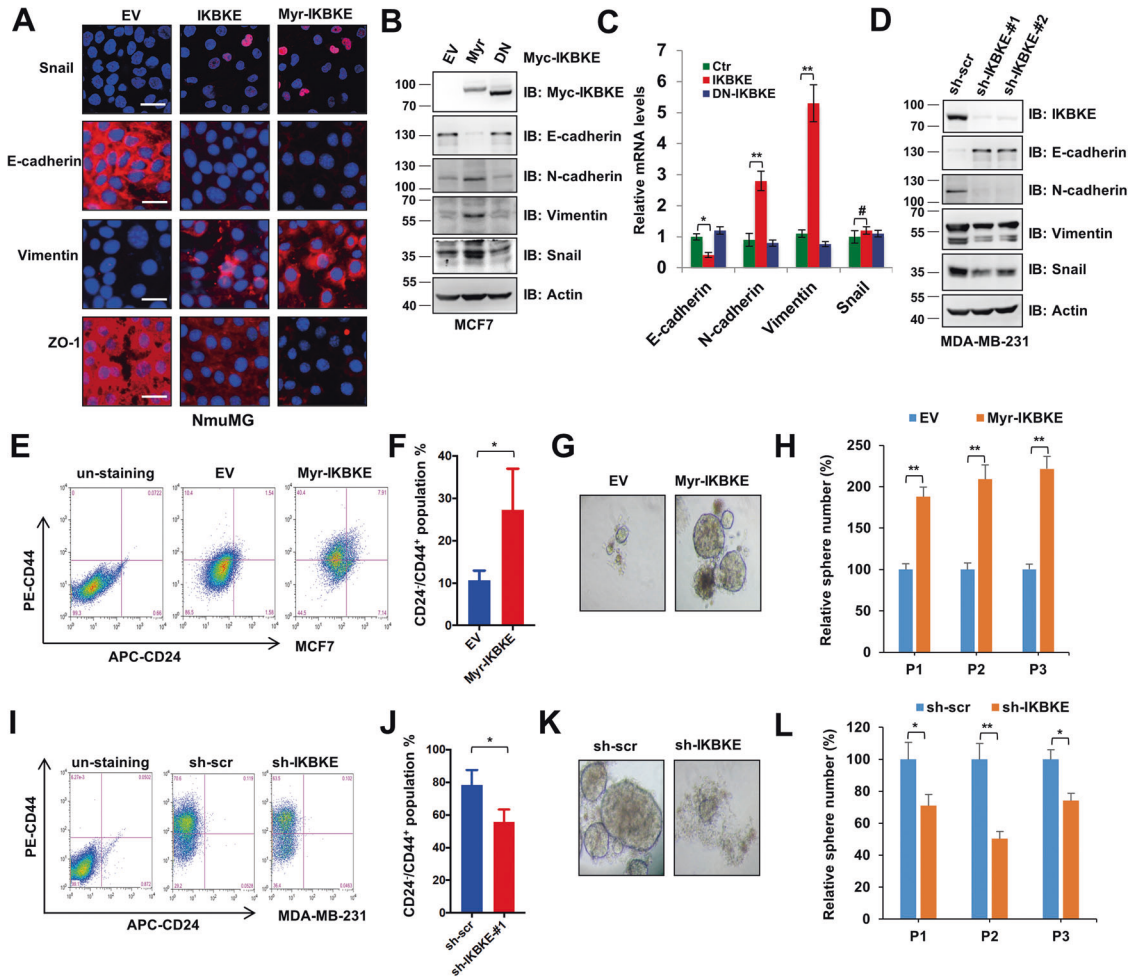

Fig. 3 IKBKE facilitates breast cell EMT and stemness. A Mouse non-transformed mammary gland epithelial cell line NmuMG was infected with IKBKE encoding virus and selected with puromycin (1 μg/ml) for 5 days and subjected to IF staining with indicated antibodies. Scale bar 20 μm. **B**, **C** MCF7 cells were infected with IKBKE encoding virus and selected with puromycin (1 μg/ml) for 5 days and harvested for IB analysis. **C** The mRNAs were obtained from the cells generated in (**B**) subjected to qRT-PCR assays. An experiment was determined in triplicated. Results were representative of three independent experiments. Data are expressed as mean ± SD. $^{\#}p > 0.05$, $^{*}p < 0.05$, $^{**}p < 0.01$ (Student *t* test). **D** MDA-MB-231 cells were infected with shRNA against *IKBKE* and selected with puromycin (1 μg/ml) for 5 days and harvested for IB analysis. **E** Cells generated in (**B**) were stained with CD24 and CD44 and subjected to flow cytometry analysis. **F** The $CD24^{-}/CD44^{+}$ cell numbers were calculated and plotted. An experiment was determined in triplicated. Results were representative of three independent experiments. Data are expressed as mean ± SD. $^{*}p < 0.05$ (Student *t* test). **G**, **H** Cells generated in (**B**) were subjected for sphere formation assays (**G**), after passage 3 generations, the sphere formation rates were calculated (**H**). The experiment was determined in triplicated. Results were representative of three independent experiments. Data are expressed as mean ± SD. $^{**}p < 0.01$ (Student *t* test). **I**, **J** Cells generated in (**D**) were stained with CD24 and CD44 antibodies and subjected to flow cytometry analysis (**I**), the $CD24^{-}/CD44^{+}$ cell numbers were calculated and plotted (**J**). An experiment was determined in triplicated. Results were representative of three independent experiments. Data are expressed as mean ± SD. $^{*}p < 0.05$ (Student *t* test). **K**, **L** Cells generated in (**D**) were subjected for sphere formation assays (**K**), after passage 3 generations, the sphere formation rates were calculated (**L**). Experiment was determined in triplicated. Results were representative of three independent experiments. Data are expressed as mean ± SD. $^{*}p < 0.05$, $^{**}p < 0.01$ (Student *t* test).

directly phosphorylate Snail (Fig. 5C, S4C–E). To identify the phosphorylated site(s), the Snail immunoprecipitants derived from cells transfected with active IKBKE individually or treatment with COMP1 were subjected to Mass Spectrometry (MS) analyses, several phosphorylation residues enhanced by IKBKE and repressed by COMP1 were selected (Figure S4F). Of note, among the detected phosphorylation residues (Fig. S4G), serine165 (S165) at Snail was identified not only conserved in other Snail members (Slug and Snail3) but also evolutionally conserved among different species, which resides in a typical IKBKE phosphorylated substrate motif (Y/P-x-p**S/T**-L/F) (Fig. 5D, E) [37]. To testify the phosphorylation at S165 of Snail, we substituted S165 to A165 (S165A-Snail) and observed that IKBKE-mediated Snail phosphorylation was largely attenuated, which were detected with both phos-tag (Figure S4H, I) and in vitro kinase assays (Fig. 5F). To detect the physiological phosphorylation of Snail, we generated antibodies against phospho-Snail-S165, which could specifically recognize pS165-Snail in a dot blot assay (Fig. S4J), and activated IKBKE could phosphorylate the S165 site of Snail (Figure S4I). More importantly, this phospho-antibody could detect the phospho-Snail in vitro kinase assays (Fig. 5G, H). Consistently, IKBKE inhibitor COMP1 could markedly abrogate IKBKE-induced Snail phosphorylation at S165 (Fig. 5I). These observations together indicate that IKBKE directly phosphorylates Snail at Ser165.

As β-TRCP1 is a well-established Snail E3 ligase and plays important roles in degradation of Snail [33], we hypothesized that IKBKE-mediated phosphorylation of Snail blocked its interaction with β-TRCP1. As a result, Myr-IKBKE dramatically diminished the ubiquitination of Snail-WT but not S165A-Snail (Fig. 5J), possibly resulted from the reason that Myr-IKBKE abrogated the binding of Snail with β-TRCP1 induced by IKBKE (Fig. 5K). Consistently, Snail-

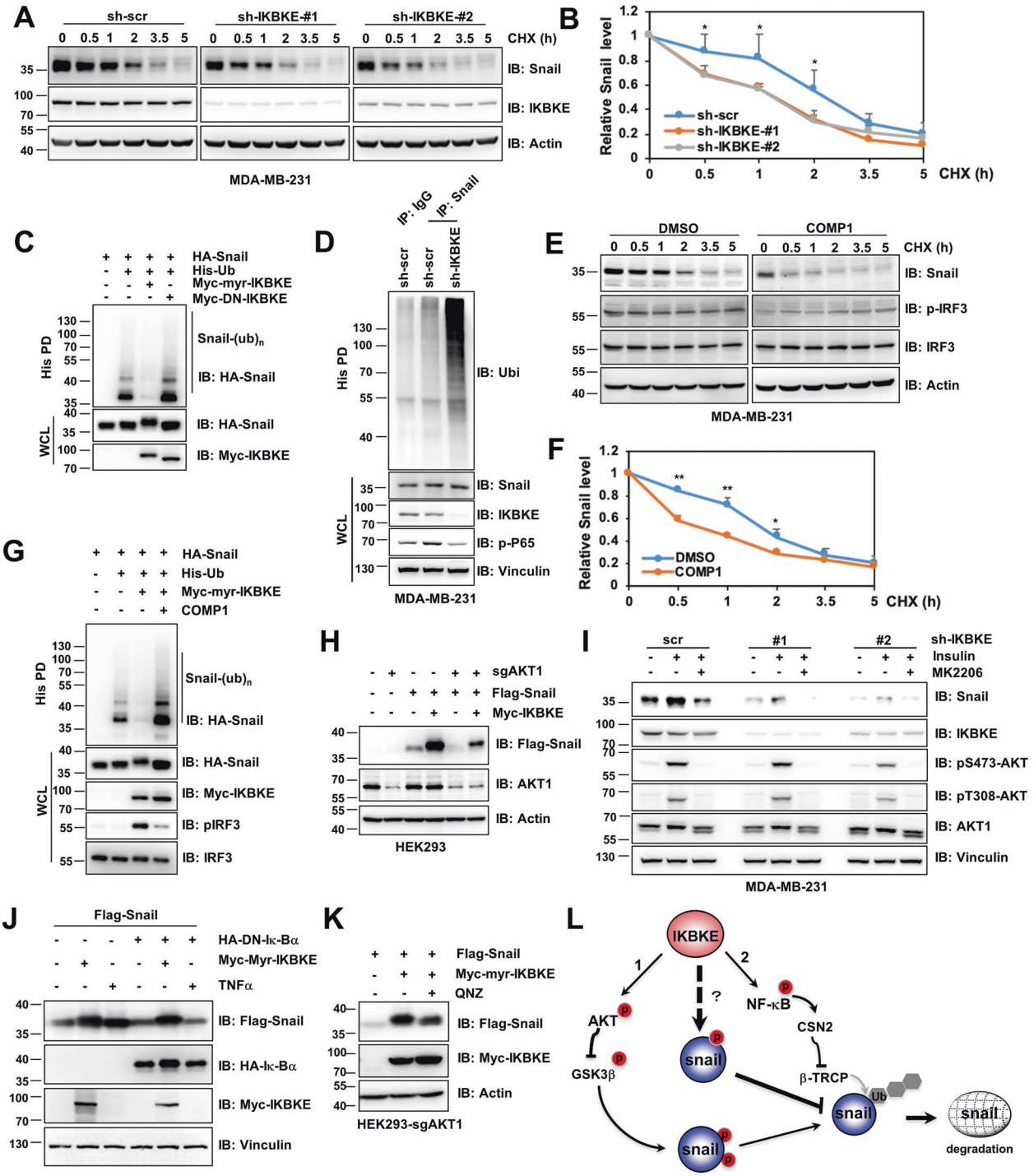

Fig. 4 IKBKE stabilized Snail partially depending on NF-κB and AKT/GSK3 pathways. A MDA-MB-231 cells infected shRNAs against *IKBKE* were treated with CHX (100 μg/ml) for indicated time course and subjected to IB analysis. **B** The relative Snail protein levels normalized with corresponding Actin was plotted. An experiment was determined in triplicated. Results were representative of three independent experiments. Data are expressed as mean ± SD. *$p < 0.05$ (Student *t* test). **C**, **G** IB analysis of whole cell lysate (WCL) and His-pull down products derived from HEK293T cells transfected with indicated constructs and treated with MG132 (10 μM) for 12 h after cells treated without (**C**) or with (**G**) IKBKE inhibitor COMP1 (5 μM) for 12 h. **D** Cells generated in (**A**) were treated with MG132 (10 μM) for 12 h and subjected to immunoprecipitated. IgG was used as a negative control. **E**, **F** MDA-MB-231 cells were administrated with COMP1 (5 μM) or DMSO overnight and further treated with CHX (100 μg/ml) for indicated time course, then subjected to IB analysis. **F** The relative Snail protein levels normalized with corresponding Actin was plotted. An experiment was determined in triplicated. Results were representative of three independent experiments. **H** CRISPR/Cas9-edited *AKT1* knockout HEK293 and parental cells were transfected with indicated constructs and subjected to IB analysis. Data are expressed as mean ± SD. *$p < 0.05$, **$p < 0.01$ (Student *t* test). **I** Cells generated in (**A**) were serum-starved for 12 h and treated with or without AKT inhibitor MK2206 (1 μM) before stimulated with insulin (0.1 μM) 5 h. The resulting cells were subjected to IB analysis with indicated antibodies. **J** HEK293T cells were transfected with indicated constructs and treated with or without TNFα (1 ng/ml) for 24 h before harvested for IB analysis. **K** *AKT1* knockout HEK293 cells were transfected with indicated constructs and treated with or without NF-κB inhibitor QNZ (10 μM) for 12 h before harvested for IB analysis. **L** Illustration of IKBKE functions in the regulation of Snail stability in multiple ways.

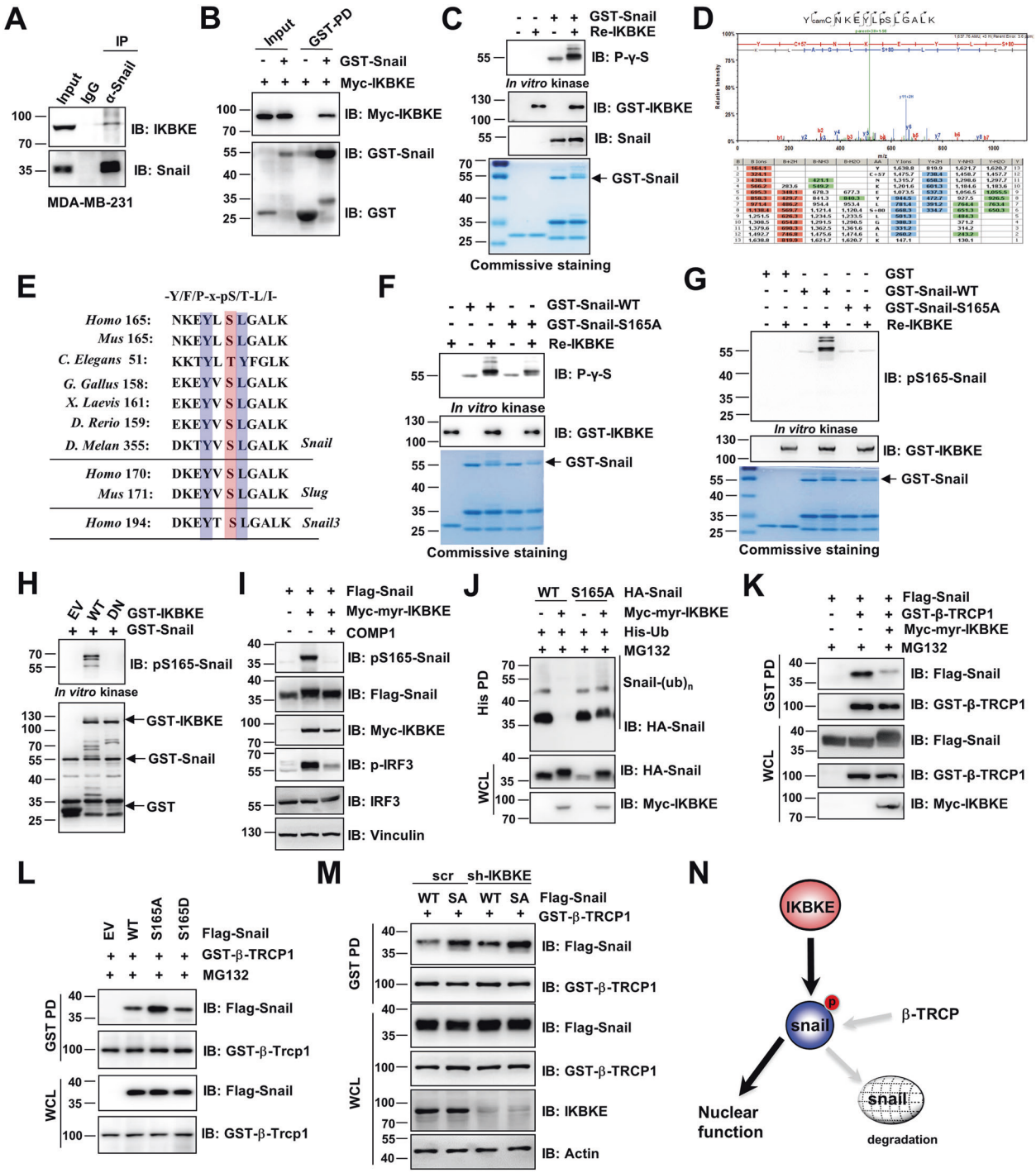

Fig. 5 IKBKE directly phosphorylates Snail. A IB analysis of WCL and IP products derived from MDA-MB-231 cells. IgG was used as negative control. **B** GST-pull down assays were performed with bacterially purified GST-Snail and WCL derived from HEK293T cells transfected with Myc-IKBKE. **C**, **D** In vitro kinase assays were performed with the recombinant IKBKE as the source of kinase and bacterially purified GST-Snail as the substrate. The kinase products were subjected to IB analysis (**C**) and mass spectrometry analysis (**D**). **E** Sequence analysis of the amino acids among different species and snail family members. Highlight is the conserved motif of putative IKBKE phosphorylation substrate as listed at the top. **F**, **G** In vitro kinase assays were performed with the recombinant IKBKE kinase and bacterially purified GST-Snail wild-type (WT) and S165A mutant. The in vitro kinase products were detected with indicated antibodies. **H** WT and DN-IKBKE were ectopically expression in HEK293T cells, and were further pulldown and subjected to in vitro kinase assays. In the kinase assays, bacterially purified GST-Snail was used as the substrate. The in vitro kinase products were subjected for IB analysis and detected with indicated antibodies. **I** IB analysis of WCL derived from HEK293T cells transfected with the indicated constructs and treated without or with COMP1 (5 μM) for 12 h. **J**–**L** IB analysis of WCL and pull-down products derived from HEK293T cells transfected with the indicated constructs and treated with MG132 (10 μM) for 12 h. M IB analysis of WCL and pull-down products derived from *IKBKE* depleted cells transfected with indicated constructs and treated with MG132 (10 μM) for 12 h. **N** Carton illustrates the role of IKBKE in regulating β-TRCP1-mediated Snail degradation by direct phosphorylation.

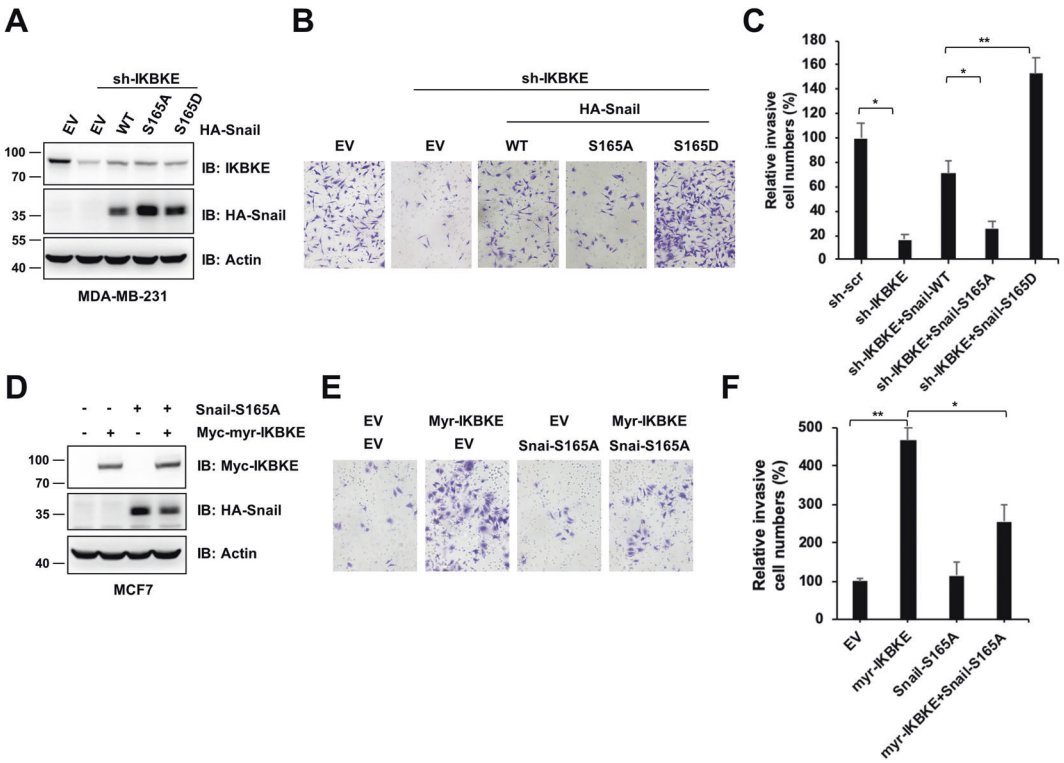

Fig. 6 Snail mediated IKBKE functions in promoting breast cancer cell invasion and migration. A MDA-MB-231 cells infected with shRNA against *IKBKE* and selected with puromycin 5 days, and further infected with Snail encoding virus and selected with hygromycin 5 days. The resulting cells were subjected to Matrigel-based invasion assays (**B**), the invasive cell numbers were calculated and plotted (**C**). The experiment was determined in triplicated. Results were representative of three independent experiments. Data are expressed as mean ± SD. *$p < 0.05$, **$p < 0.01$ (Student *t* test). **D** MCF7 cells infected with indicated encoding virus, and selected with puromycin for IKBKE and hygromycin for Snail-S165 respectively. **E** Resulting cells were subjected to Matrigel-based invasion assays, the invasive cell numbers were calculated and plotted (**F**). The experiment was determined in triplicated. Results were representative of three independent experiments. Data are expressed as mean ± SD. *$p < 0.05$, **$p < 0.01$ (Student *t* test).

S165A markedly elevated the interaction of Snail with β-TRCP1 (Fig. 5L). Moreover, *IKBKE* depletion enhanced the interaction of β-TRCP1 and Snail (Fig. 5M), suggesting that IKBKE stabilizes Snail through phosphorylating Snail and blocking its interaction with the E3 ligase β-TRCP1 (Fig. 5N).

Snail mediates IKBKE functions in promoting breast cancer cell invasion and migration

A plethora of proteins has been reported as bona fide substrates of IKBKE to mediate its malignancies [16]. Based on the pivotal roles of Snail in promoting invasion and migration, we sought to detect whether IKBKE-mediated Snail phosphorylation contributed to its roles in promoting breast cancer cell invasion and migration. To this end, WT, non-phospho-mimic mutant S165A, and phospho-mimic mutant S165D were ectopically expressed in *IKBKE*-deficient MDA-MB-231 cells (Fig. 6A). We observed that *IKBKE* depletion-reduced cellular invasion and migration was markedly rescued by ectopic expression of S165D-Snail, but only mildly rescued by S165A-Snail (Fig. 6B, C, S5A, B). On the other hand, S165A-Snail was also ectopically expressed (Fig. 6D), which could robustly repress Myr-IKBKE-induced MCF7 invasion and migration (Fig. 6E, F, S5C, D). These findings together suggest that phosphorylation of Snail at S165 is critical for IKBKE-mediated breast cancer invasion and migration.

IKBKE expression is correlated with Snail phosphorylation at S165 and breast cancer lymph node metastasis

To assess the clinical relevance of IKBKE, we initially detected the expression of IKBKE and Snail in breast cancer tissues. The results showed that high expression of IKBKE was positively correlated with Snail protein levels (Fig. 7A). Furthermore, we performed IHC staining for IKBKE and pS165-Snail in a human breast cancer tissue microarray (TMA), and observed that, compared to carcinoma in situ (CIS), IKBKE exhibited higher expression in invasive carcinoma (IC) with lymph node metastasis (Fig. 7B). Furthermore, the expression of IKBKE was significantly correlated with pS165-Snail (Fig. 7C). Meanwhile, pS165-Snail was also mainly detected in lymph node metastasis IC samples (Fig. 7D). Importantly, both IKBKE and pS165-Snail were markedly correlated with breast cancer lymph node (L.N.) migration (Fig. 7D). Database analyses also suggest that high expression of IKBKE and Snail were both correlated with poor survival in lymph node-positive breast cancer patients, while IKBKE did not act as a biomarker for lymph node-negative breast cancer patients (Fig. S6A–D). These findings together indicate that IKBKE plays an important role in promoting breast cancer metastasis by phosphorylating Snail, and will be considered as a breast cancer lymph node migration biomarker.

DISCUSSION

MMTV-PyVMT mouse model is well established to investigate human breast tumorigenesis, particularly for the mammary tumor lung metastasis [48]. Although mildly affecting mammary development in wild-type mice, depleting *Ikbke* could dramatically compromise the mammary neoplasia development, tumor growth, and further mammary tumor lung metastasis in the *MMTV-PyVMT* mouse model (Fig. 1). While, previous and our results have shown that *Ikbke* deficiency could markedly impair breast cancer cell fitness, resulting in reduced mammary tumor growth which has been considered as a major cause of influencing

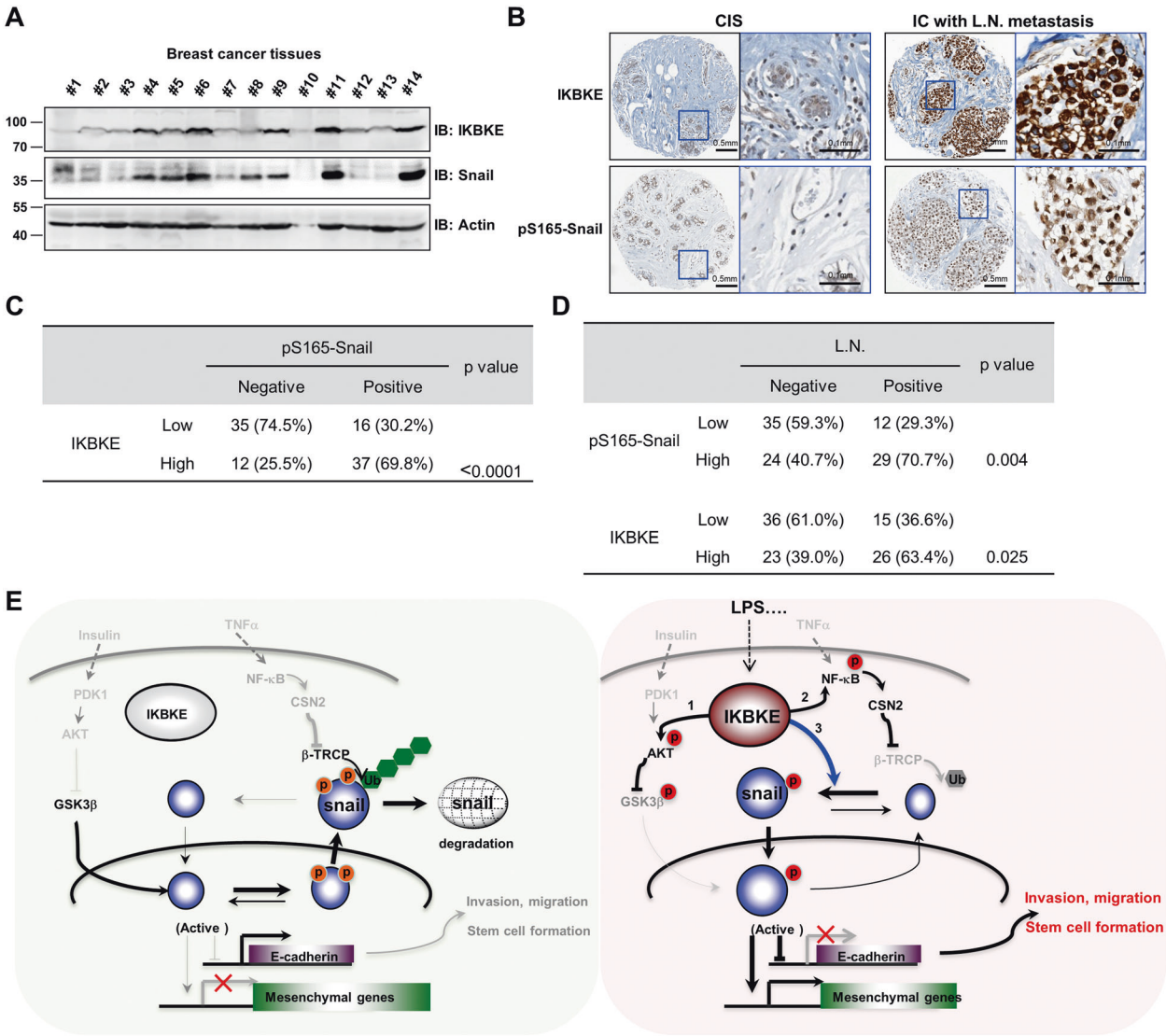

Fig. 7 IKBKE is associated with breast tumor metastasis. A IB analysis of WCL derived from breast cancer tissues. **B** Images represent the IHC staining of indicated antibodies in CIS (carcinoma in situ) and IC (invasive carcinoma) with lymph node metastasis. **C** The correlation of IKBKE and pS165-Snail staining in (**B**) were analyzed and tabled. **D** The distribution of IKBKE and pS165-Snail staining in lymph node metastasis IC was calculated and tabled. **E** Illustration of IKBKE functions in regulating Snail stability in distinct ways. Under normal conditions, Snail was phosphorylated by GSK3β, and recognized by β-TRCP for ubiquitination and subsequent degradation to keep cell epithelial phenotype (left panel). In contrast, under conditions of LPS or other stimulations, or amplification of *IKBKE*, the active IKBKE could (1) inhibit GSK3β-mediated Snail phosphorylation, (2) activate NF-κB-mediated regulation of β-TRCP, and (3) directly phosphorylate Snail, and further enhances Snail stability and contributes to invasion and migration phenotypes.

mammary tumor metastasis [11]. On the other hand, IKBKE also exhibits profound roles in re-modulating the lung inflammatory and immune-microenvironments which would also largely contribute to mammary tumor lung metastasis [24]. To exclude these possibilities, we employed another well-established xenograft mouse model via tail vein injecting the tumor cells, which could potently measure the capability of tumor cell lung residence. From in vivo mouse model and in vitro cellular studies, we reveal that IKBKE indeed facilitates breast cancer lung metastasis. However, to further exclude the immunological effects for IKBKE-mediated mammary tumor lung metastasis, the syngeneic mouse models will be employed, in which the mouse mammary tumor cell lines would be used to perform lung metastatic assays in both *Ikbke*$^{-/-}$ and counterpart mice. In addition, *Ikbke* mammary conditional knockout mouse model is worth to be engineered and consequently crossed with *Erbb2* or *Myc* transgenic mice to prove the potent role of IKBKE in mediating mammary tumor growth and lung metastasis.

It is well acknowledged that tumor microenvironments provide a specific niche for tumor invasion and migration [49]. Under physiological conditions, the presence of insulin or other growth factors would activate AKT pathway and mediate the phosphorylation and repression of GSK3β to abrogate its function in phosphorylating and degrading Snail (Fig. 7E). On the other hand, the presence of TNFα or other cytokines could efficiently activate NF-κB pathway to disturb CSN2 protein and block β-TRCP-mediate Snail ubiquitination and degradation (Fig. 7E). Strikingly, although IKBKE has been revealed to directly govern AKT/GSK3β and NF-κB/CSN2 pathways for manipulating Snail abundance under distinct conditions, another critical role of IKBKE in regulating Snail have also been experimentally proved by directly phosphorylating Snail, which disturbs Snail ubiquitination and degradation (Fig. 4).

Pathologically, *IKBKE* is not only genetically amplified in many types of cancer, such as breast and lung cancers [11, 21], but also could be induced by inflammatory factors or cytokines, such as LPS, PMA [17, 18], to promote Snail stability, leading to breast cancer EMT, invasion, and metastasis. Therefore, our findings implicate that aberrant expression/activation of IKBKE could directly phosphorylate and stabilize Snail, resulting in Snail-mediated EMT-related malignancies and accounting for breast cancer metastasis.

Accumulating substrates of IKBKE have been identified recently, all of which together contribute to inflammation and tumorigenesis. Among these substrates, such as YAP and STAT3, have been reported to control cancer cell metastasis [15, 24]. However, the potential functions and underlying mechanisms of IKBKE involved in mammary cancer lung metastasis are not well defined yet. Here we demonstrate that IKBKE could robustly stabilize Snail to control EMT, sustain stemness, and acquire invasive phenotypes of breast cancer cell. However, whether other IKBKE substrates, except AKT and NF-κB, could confer IKBKE roles in promoting breast cancer EMT and lung metastasis are desired to be further investigated. In summary, we demonstrate that depletion of *Ikbke* could compromise mammary tumorigenesis and lung metastasis in an *MMTV-PyVMT* mouse model. We further confirm that IKBKE could trigger human breast cancer cell EMT phenotype, resulting in promoting cancer cell migration, invasion. Mechanically, IKBKE could not only regulate Snail by modulating AKT/GSKβ and NF-κB/CSN2 pathways, but also directly phosphorylate Snail to prevent its degradation. Thus, our study reveals a crucial role for IKBKE in accelerating breast tumor metastasis, and highlights a potential strategy for combating breast cancer metastasis by targeting IKBKE kinase.

DATA AVAILABILITY

No data was uploaded to the public database. All the data were available upon rational request.

REFERENCES

1. Siegel RL, Miller KD, Jemal A. Cancer statistics, 2020. CA Cancer J Clin. 2020;70:7–30.
2. Mettlin C. Global breast cancer mortality statistics. CA Cancer J Clin. 1999;49:138–44.
3. Chuang HY, Lee E, Liu YT, Lee D, Ideker T. Network-based classification of breast cancer metastasis. Mol Syst Biol. 2007;3:140.
4. Dent R, Trudeau M, Pritchard KI, Hanna WM, Kahn HK, Sawka CA, et al. Triple-negative breast cancer: Clinical features and patterns of recurrence. Clin Cancer Res. 2007;13:4429–34.
5. Ramaswamy S, Ross KN, Lander ES, Golub TR. A molecular signature of metastasis in primary solid tumors. Nat Genet. 2003;33:49–54.
6. Weigelt B, Glas AM, Wessels LF, Witteveen AT, Peterse JL, van't Veer LJ. Gene expression profiles of primary breast tumors maintained in distant metastases. Proc Natl Acad Sci USA. 2003;100:15901–5.
7. Coussens LM, Werb Z. Inflammation and cancer. Nature. 2002;420:860–7.
8. Berasain C, Castillo J, Perugorria MJ, Latasa MU, Prieto J, Avila MA. Inflammation and liver cancer: New molecular links. Ann NY Acad Sci. 2009;1155:206–21.
9. Fox JG, Wang TC. Inflammation, atrophy, and gastric cancer. J Clin Invest. 2007;117:60–9.
10. Arkan MC, Greten FR. IKK- and NF-kappaB-mediated functions in carcinogenesis. Curr Top Microbiol Immunol. 2011;349:159–69.
11. Boehm JS, Zhao JJ, Yao J, Kim SY, Firestein R, Dunn IF, et al. Integrative genomic approaches identify IKBKE as a breast cancer oncogene. Cell. 2007;129:1065–79.
12. Barbie DA, Tamayo P, Boehm JS, Kim SY, Moody SE, Dunn IF, et al. Systematic RNA interference reveals that oncogenic KRAS-driven cancers require TBK1. Nature. 2009;462:108–12.
13. Ou YH, Torres M, Ram R, Formstecher E, Roland C, Cheng T, et al. TBK1 directly engages Akt/PKB survival signaling to support oncogenic transformation. Mol Cell. 2011;41:458–70.
14. Xie X, Zhang D, Zhao B, Lu MK, You M, Condorelli G, et al. IkappaB kinase epsilon and TANK-binding kinase 1 activate AKT by direct phosphorylation. Proc Natl Acad Sci USA. 2011;108:6474–9.
15. Wang S, Xie F, Chu F, Zhang Z, Yang B, Dai T, et al. YAP antagonizes innate antiviral immunity and is targeted for lysosomal degradation through IKKvarepsilon-mediated phosphorylation. Nat Immunol. 2017;18:733–43.
16. Durand JK, Zhang Q, Baldwin AS. Roles for the IKK-Related Kinases TBK1 and IKKepsilon in Cancer. Cells. 2018;7:139.
17. Shimada T, Kawai T, Takeda K, Matsumoto M, Inoue J, Tatsumi Y, et al. IKK-i, a novel lipopolysaccharide-inducible kinase that is related to IkappaB kinases. Int Immunol. 1999;11:1357–62.
18. Peters RT, Liao SM, Maniatis T. IKKepsilon is part of a novel PMA-inducible IkappaB kinase complex. Mol Cell. 2000;5:513–22.
19. Sankar S, Chan H, Romanow WJ, Li J, Bates RJ. IKK-i signals through IRF3 and NFkappaB to mediate the production of inflammatory cytokines. Cell Signal. 2006;18:982–93.
20. Tenoever BR, Ng SL, Chua MA, McWhirter SM, Garcia-Sastre A, Maniatis T. Multiple functions of the IKK-related kinase IKKepsilon in interferon-mediated antiviral immunity. Science. 2007;315:1274–8.
21. Challa S, Guo JP, Ding X, Xu CX, Li Y, Kim D, et al. IKBKE Is a Substrate of EGFR and a therapeutic target in non-small cell lung cancer with activating mutations of EGFR. Cancer Res. 2016;76:4418–29.
22. Guo JP, Shu SK, He L, Lee YC, Kruk PA, Grenman S, et al. Deregulation of IKBKE is associated with tumor progression, poor prognosis, and cisplatin resistance in ovarian cancer. Am J Pathol. 2009;175:324–33.
23. Shen RR, Zhou AY, Kim E, Lim E, Habelhah H, Hahn WC. IkappaB kinase epsilon phosphorylates TRAF2 to promote mammary epithelial cell transformation. Mol Cell Biol. 2012;32:4756–68.
24. Barbie TU, Alexe G, Aref AR, Li S, Zhu Z, Zhang X, et al. Targeting an IKBKE cytokine network impairs triple-negative breast cancer growth. J Clin Invest. 2014;124:5411–23.
25. Zhao Z, Li Y, Liu H, Jain A, Patel PV, Cheng K. Co-delivery of IKBKE siRNA and cabazitaxel by hybrid nanocomplex inhibits invasiveness and growth of triple-negative breast cancer. Sci Adv. 2020;6:eabb0616.
26. Lu W, Kang Y. Epithelial-mesenchymal plasticity in cancer progression and metastasis. Dev Cell. 2019;49:361–74.
27. Ye X, Weinberg RA. Epithelial-mesenchymal plasticity: A central regulator of cancer progression. Trends Cell Biol. 2015;25:675–86.
28. Ye X, Tam WL, Shibue T, Kaygusuz Y, Reinhardt F, Ng Eaton E, et al. Distinct EMT programs control normal mammary stem cells and tumour-initiating cells. Nature. 2015;525:256–60.
29. Mani SA, Guo W, Liao MJ, Eaton EN, Ayyanan A, Zhou AY, et al. The epithelial-mesenchymal transition generates cells with properties of stem cells. Cell. 2008;133:704–15.
30. Barrallo-Gimeno A, Nieto MA. The Snail genes as inducers of cell movement and survival: Implications in development and cancer. Development. 2005;132:3151–61.
31. Zhang JP, Zeng C, Xu L, Gong J, Fang JH, Zhuang SM. MicroRNA-148a suppresses the epithelial-mesenchymal transition and metastasis of hepatoma cells by targeting Met/Snail signaling. Oncogene. 2014;33:4069–76.
32. Bai X, Geng J, Zhou Z, Tian J, Li X. MicroRNA-130b improves renal tubulointerstitial fibrosis via repression of Snail-induced epithelial-mesenchymal transition in diabetic nephropathy. Sci Rep. 2016;6:20475.
33. Zhou BP, Deng J, Xia W, Xu J, Li YM, Gunduz M, et al. Dual regulation of Snail by GSK-3beta-mediated phosphorylation in control of epithelial-mesenchymal transition. Nat Cell Biol. 2004;6:931–40.
34. Yang Z, Rayala S, Nguyen D, Vadlamudi RK, Chen S, Kumar R. Pak1 phosphorylation of snail, a master regulator of epithelial-to-mesenchyme transition, modulates snail's subcellular localization and functions. Cancer Res. 2005;65:3179–84.
35. Du C, Zhang C, Hassan S, Biswas MH, Balaji KC. Protein kinase D1 suppresses epithelial-to-mesenchymal transition through phosphorylation of snail. Cancer Res. 2010;70:7810–9.
36. Guo J, Dai X, Laurent B, Zheng N, Gan W, Zhang J, et al. AKT methylation by SETDB1 promotes AKT kinase activity and oncogenic functions. Nat Cell Biol. 2019;21:226–37.
37. Hutti JE, Shen RR, Abbott DW, Zhou AY, Sprott KM, Asara JM, et al. Phosphorylation of the tumor suppressor CYLD by the breast cancer oncogene IKKepsilon promotes cell transformation. Mol Cell. 2009;34:461–72.
38. Allen JJ, Li M, Brinkworth CS, Paulson JL, Wang D, Hubner A, et al. A semisynthetic epitope for kinase substrates. Nat Methods. 2007;4:511–6.
39. Zhang J, Guo J, Qin X, Wang B, Zhang L, Wang Y, et al. The p85 isoform of the kinase S6K1 functions as a secreted oncoprotein to facilitate cell migration and tumor growth. Sci Signal. 2018;11:eaao1052.
40. Jenkins RW, Aref AR, Lizotte PH, Ivanova E, Stinson S, Zhou CW, et al. Ex vivo profiling of PD-1 blockade using organotypic tumor spheroids. Cancer Disco. 2018;8:196–215.

41. Morel AP, Lievre M, Thomas C, Hinkal G, Ansieau S, Puisieux A. Generation of breast cancer stem cells through epithelial-mesenchymal transition. PLoS One. 2008;3:e2888.
42. Orlova Z, Pruefer F, Castro-Oropeza R, Ordaz-Ramos A, Zampedri C, Maldonado V, et al. IKKepsilon regulates the breast cancer stem cell phenotype. Biochim Biophys Acta Mol Cell Res. 2019;1866:598–611.
43. Ricardo S, Vieira AF, Gerhard R, Leitao D, Pinto R, Cameselle-Teijeiro JF, et al. Breast cancer stem cell markers CD44, CD24 and ALDH1: Expression distribution within intrinsic molecular subtype. J Clin Pathol. 2011;64:937–46.
44. Wu Y, Deng J, Rychahou PG, Qiu S, Evers BM, Zhou BP. Stabilization of snail by NF-kappaB is required for inflammation-induced cell migration and invasion. Cancer Cell. 2009;15:416–28.
45. Cross DA, Alessi DR, Cohen P, Andjelkovich M, Hemmings BA. Inhibition of glycogen synthase kinase-3 by insulin mediated by protein kinase B. Nature. 1995;378:785–9.
46. Moreno R, Sobotzik JM, Schultz C, Schmitz ML. Specification of the NF-kappaB transcriptional response by p65 phosphorylation and TNF-induced nuclear translocation of IKK epsilon. Nucleic Acids Res. 2010;38:6029–44.
47. Connelly L, Barham W, Onishko HM, Sherrill T, Chodosh LA, Blackwell TS, et al. Inhibition of NF-kappa B activity in mammary epithelium increases tumor latency and decreases tumor burden. Oncogene. 2011;30:1402–12.
48. Denzel MS, Hebbard LW, Shostak G, Shapiro L, Cardiff RD, Ranscht B. Adiponectin deficiency limits tumor vascularization in the MMTV-PyV-mT mouse model of mammary cancer. Clin Cancer Res. 2009;15:3256–64.
49. Rohan TE, Xue X, Lin HM, D'Alfonso TM, Ginter PS, Oktay MH, et al. Tumor microenvironment of metastasis and risk of distant metastasis of breast cancer. J Natl Cancer Inst. 2014;106:dju136.

ACKNOWLEDGEMENTS

We thank the members of the Guo laboratory for critical reading and kind suggestions of the paper. We thank Yilin Li, Ping Wu, and Chao Peng in National Facility for Protein Science in Shanghai for Mass Spectrometry analysis. This work was supported by China National Nature Science Foundation (J.G. 31871410, 32070767; Q.J. 32100559)

AUTHOR CONTRIBUTIONS

This study was conceived and designed by JG, WX. Development of methodology: JG, WX, QJ, XW, and LW. Acquisition of data (provided animals, acquired and managed patients, provided facilities, etc.): JG, QH, WX, QJ, LW, XW, BG, and YL. Analysis and interpretation of data (e.g., statistical analysis, biostatistics, computational analysis): JG, WX, and LW. Revision of the paper: WX, QJ, XW, LW, and YL. Writing the paper: JG, WX. Administrative, technical, or material support (i.e., reporting or organizing data, constructing databases): QJ, LW, XW, ZS, XZ, and LB. Study supervision: JG, JL. Approved paper: all authors.

COMPETING INTERESTS

The authors declare no competing interests.

ETHICS STATEMENT

All procedures followed are in accordance with the ethical standards approved by the Institutional Animal Care and Use Committee of Sun Yat-sen University.

ADDITIONAL INFORMATION

Supplementary information The online version contains supplementary material available at https://doi.org/10.1038/s41418-022-00940-1.

Correspondence and requests for materials should be addressed to Qiang Huang, Jie Li or Jianping Guo.